



New insights into comparison between synthetic and practical municipal wastewater in cake layer characteristic analysis of membrane bioreactor



Lijie Zhou^{a,b,*}, Wei-Qin Zhuang^c, Xin Wang^d, Ke Yu^e, Shufang Yang^f, Siqing Xia^d

^a College of Chemistry and Environmental Engineering, Shenzhen University, Shenzhen 518060, PR China

^b Shenzhen Academy of Environmental Sciences, Shenzhen 518001, PR China

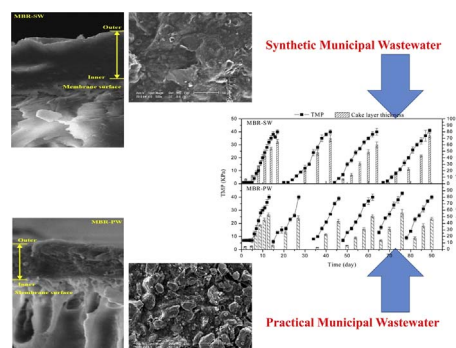
^c Department of Civil and Environmental Engineering, University of Auckland, Auckland 1142, New Zealand

^d State Key Laboratory of Pollution Control and Resource Reuse, College of Environmental Science and Engineering, Tongji University, 1239 Siping Road, Shanghai 200092, PR China

^e School of Environment and Energy, Peking University Shenzhen Graduate School, Shenzhen 518055, PR China

^f Shenzhen Municipal Design & Research Institute Co., Ltd, 3007 West Sungang Road, Shenzhen 518029, PR China

GRAPHICAL ABSTRACT



ARTICLE INFO

Keywords:

Synthetic municipal wastewater
Practical municipal wastewater
Cake layer
Membrane bioreactor

ABSTRACT

In previous studies, cake layer analysis in membrane bioreactor (MBR) was both carried out with synthetic and practical municipal wastewater (SMW and PMW), leading to different results. This study aimed to identify the comparison between SMW and PMW in cake layer characteristic analysis of MBR. Two laboratory-scale anoxic/oxic MBRs were operated for over 90 days with SMW and PMW, respectively. Results showed that PMW led to rough cake layer surface with particles, and the aggravation of cake layer formation with thinner and denser cake layer. Additionally, inorganic components, especially Si and Al, in PMW accumulated into cake layer and strengthened the cake layer structure, inducing severer biofouling. However, SMW promoted bacterial metabolism during cake layer formation, thus aggravated the accumulation of organic components into cake layer. Therefore, SMW highlighted the organic components in cake layer, but weakened the inorganic functions in practical MBR operation.

* Corresponding author at: College of Chemistry and Environmental Engineering, Shenzhen University, Shenzhen 518060, PR China.
E-mail addresses: pakerzhou@gmail.com, pakerzhou@szu.edu.cn (L. Zhou).

1. Introduction

Membrane bioreactor (MBR) is considered as a well-established, mature technology in recent decades, and has been widely applied in many full-scale plants for municipal and industrial wastewater treatment (Deng et al., 2016; Huang and Lee, 2015; Jegatheesan et al., 2016). MBR could achieve high nutrient removal efficiency with complete biomass retention, totally separating hydraulic retention time (HRT) and solids retention time (SRT). Thus, increasing interest in MBR application has been shown in China wastewater treatment market (Meng et al., 2017). Total treatment capacity of large-scale MBRs was over 1.0 million m³/d, and it is expected that the capacity will over 10.0 million m³/d in 2017 (Xiao et al., 2014). Although MBR contains plenty of outstanding advantages, such as complete retention of sludge, high quality of effluent, low footprint, membrane biofouling and its cake layer still remain serious operational obstacles and challenges in the wider spread of MBR (Duan et al., 2013; Tian and Su, 2012; Xia et al., 2008).

During 2010–2015, approximate 600–700 research literatures were published per year related to wastewater treatment with MBRs, and approximate 22% papers were about membrane biofouling and its cake layer (Meng et al., 2017). Cake layer characteristic analysis is regarded as the foundation for understanding the cake layer formation mechanism to carry out novel biofouling mitigation methods (Deng et al., 2016; Gkotsis et al., 2017; Huang and Lee, 2015). Organic components, especially extracellular substances (ES), is considered as the majority of cake layer, and lots of studies are focus on the polysaccharide, protein, humic substances, etc. in ES and their relationship with cake layer (Ng et al., 2010; Ou et al., 2010; Wang et al., 2009). Polysaccharide has been identified as the dominate biopolymers (> 100 kDa) and also the key biofouling-causing substance during low-pressure filtration (Meng et al., 2017). In addition, protein and humic substance are deemed making biofouling and cake layer structure more complex (Liu et al., 2011; Meng et al., 2017). Thus, many biofouling mitigation methods have been carried out to reduce the organic biofouling during MBR operation, such as sludge control, quorum quenching, nanocomposite membrane, etc. (Homayoonfal et al., 2015; Jiang et al., 2013; Meng et al., 2017). However, the studies for cake layer characteristic analysis were operated with different wastewater, especially synthetic and practical municipal wastewater (SMW and PMW) (Campo et al., 2017; Gkotsis et al., 2017; Gurung et al., 2017). Huang and Goel (2015) has pointed out that different performance would be induced in wastewater treatment system with SMW and PMW, respectively. Additionally, recent literatures (Dang et al., 2014; Du et al., 2017; Zhou et al., 2015) have found that inorganic components, especially Si, Al, Ca, Mg, etc., play the significant role (such as the framework for cake layer structure) in the cake layer. SMW ignored inorganic components in practical MBR operation, leading to understanding variations on cake layer structure and its formation mechanism. Therefore, Villain et al. (2014) has been carried out the study on the comparison between SMW and PMW for MBR performance and membrane biofouling. However, the comparison between SMW and PMW in cake layer characteristic analysis is still unclear and needs further study.

This study aims to develop the new insights into the comparison between SMW and PMW in cake layer characteristic analysis of MBR. Two anoxic/oxic MBRs were operated for over 90 days with SMW and PMW, respectively. Cake layer characteristic were identified through cake layer morphology, organic characteristics and inorganic characteristics with ES analysis, SEM-EDX (scanning electron microscopy-energy dispersive X-ray analyzer), X-ray photoelectron spectroscopy (XPS), etc. in this study.

Table 1

Average characteristics of the influent and the effluent water of MBR-SW and MBR-PW ($n = 30$).

	MBR-SW ^a		MBR-PW ^b	
	Influent	Effluent	Influent	Effluent
COD _{Cr}	200 ± 10	7 ± 5	180 ± 60	11 ± 6
NH ₄ ⁺ -N	30 ± 1	1 ± 1	28 ± 3	1.3 ± 1
TN	35 ± 2	8 ± 2	34 ± 3	12 ± 2
TP	5 ± 1	1.8 ± 0.4	4.7 ± 1.8	2.1 ± 0.5
Ca ^c	40 ± 4	35 ± 1	110 ± 4	40 ± 3
Mg ^c	7 ± 3	5 ± 1	13 ± 2	8 ± 2
Al ^c	2 ± 1	1 ± 1	12 ± 13	0 ± 0
Si ^c	1 ± 1	0 ± 0	360 ± 40	30 ± 5

^a MBR-SW: MLSS = 4.6 g/L, MLVSS = 3.9 g/L, MLVSS/MLSS = 84%.

^b MBR-PW: MLSS = 4.0 g/L, MLVSS = 2.7 g/L, MLVSS/MLSS = 68%.

^c Influent of each element indicated its total concentration in the influent. Due to the separation performed by the membrane, all reported elements in the effluent were in the soluble fraction.

2. Materials and methods

2.1. Reactor set-up and operation

Two laboratory-scale anoxic/oxic MBRs (4.5 L working volume with 1.5 L anoxic tank and 3 L oxic tank) were operated for 90 days with SMW (MBR-SW) and PMW (MBR-PW), respectively. SMW was composed with tap water, containing 200 mg/L glucose, 200 mg/L corn starch, 10 mg/L peptone, 102.75 mg/L NH₄Cl and 40 mg/L KH₂PO₄ as well as trace nutrients such as CaCl₂ (8 mg/L), MgSO₄·7H₂O (9 mg/L), MnSO₄·H₂O (3.66 mg/L) and FeSO₄·7H₂O (0.55 mg/L) (SMW characteristics showed in Table 1; influent was adjusted with NaHCO₃ at pH 7.0) (Zhou et al., 2014). PMW was applied with the effluent from an aerated grit chamber of Quyang municipal wastewater treatment plant (WWTP) (Shanghai, China; PMW characteristics are showed in Table 1).

A polyvinylidene fluoride hollow fiber membrane module (pore size 0.4 μm; 200 dm² total surface area; manufactured by Li-tree Company, Suzhou, China) was immersed in each MBR. A constant fluid flux was maintained at 17 L/(m² h) with an intermittent suction mode (10 min on/2 min off for each cycle). 0.4 m³/h air was supplied continuously through a cross-flow diffuser. Trans-membrane pressure (TMP) was monitored with a pressure gauge. HRT and SRT were kept at 10 h and 30 days, respectively. The flow rate of recycled mixed liquor from the oxic tank to the anoxic tank was controlled at 200% of the influent flow rate. Inoculating sludge was collected from the return activated sludge stream in the Quyang WWTP (Shanghai, China). The newly inoculated A/O-MBR was initially operated to achieve steady state for sludge acclimatization. Membrane module was then replaced with a new and similar unit for the experiment. When TMP reached 40 kPa, the membrane module was cleaned with physical (washing with tap water) and chemical methods (2% NaClO followed by 1% citric acid immersion, each for 4 h prior to the next run). Basic operational information of MBRs are showed in Table 1.

2.2. Extracellular substances (ES) in cake layer

ES in cake layer was extracted based on the modified thermal extraction method (Zhou et al., 2014). The cake layer was scraped from membrane surface and dissolved in 40 mL 0.9% NaCl. Solution was treated with ultrasound (DS510DT, 40 kHz, 300W, Shangchao, China) for 8 min, then shaken at 150 rpm for 10 min. Solution was next heated at 80 °C for 30 min and centrifuged at 12,000g (MILTIFUGE X1R, Thermo Electron Corporation, USA) for 20 min. Supernatant was considered as ES of cake layer. Polysaccharide and protein are regarded as the significant roles in ES of cake layer (Deng et al., 2016).

Polysaccharide and protein were measured with the phenol-sulfuric acid method and Branford method, respectively. Three-dimensional excitation-emission (EEM) fluorescence spectra of ES in cake layer were measured via a fluorescence spectrophotometer (FluoroMax-4, HORIBA, Japan). EEM spectra were measured with the scanning emission spectra from 200 nm to 550 nm at 5 nm increments by varying the excitation wavelengths from 200 nm to 500 nm at 5 nm sampling intervals.

2.3. Inorganic elements concentrations

Concentrations of inorganic elements in the influent, effluent and cake layer were analyzed with an inductively coupled plasma-optical emission spectrometer (ICP-OES, Optima 2100 DV, Perkin Elmer, USA) according to the Standard Methods (China-NEPA, 2002).

2.4. XPS measurement

The sample was scraped from the fouled membrane modules and freeze-dried for 48 h prior to XPS (PHI-5000C ESCA, Perkin Elmer, USA) analysis described in Zhou et al. (2015). XPS data was analyzed using the software of Auger Scan 320 Demo.

2.5. SEM-EDX (scanning electron microscopy-energy-dispersive X-ray analyzer) analysis

A piece of the membrane fiber was cut from the middle part of the membrane module after frozen in liquid-nitrogen. Membrane fiber was analyzed with SEM (XL30, Philips, Netherlands) coupled with an EDX (Oxford Isis, UK).

2.6. Other analytical methods

Determination of chemical oxygen demand (COD_{Cr}), ammonia nitrogen (NH₄⁺-N), total phosphorus (TP), total nitrogen (TN) and mixed liquid suspended solid (MLSS) were conducted in accordance with Standard Methods (China-NEPA, 2002). Dissolved oxygen (DO) and pH were identified with DO-pH analyzer (HQ4d, HACH, USA). Molecular weight (MW) distribution of ES in cake layer was measured with a gel filtration chromatography (GFC; with a TSK G4000SW type gel column (TOSOH Corporation, Japan) and a liquid chromatography spectrometer (LC-10ATVP, SHIMADZU, Japan)) analyzer. Viscosity of cake layer was identified with DV-C viscometer (Brookfield, USA).

2.7. Statistical analysis

Person's product momentum correlation coefficient (r_p , Eq. (1)) was carried out for the linear correlation between two parameters.

$$r_p = \frac{\sum (x - x_{avg})(y - y_{avg})}{\sqrt{\sum (x - x_{avg})^2 \sum (y - y_{avg})^2}} \quad (1)$$

where (x, y) is a sample of paired data, and x_{avg} and y_{avg} are mean value. Value of r_p oscillate between -1 and +1, as $r_p = -1$ or $r_p = +1$ indicates a perfect correlation, and 0 showed no correlation. If $-0.4 < r_p < +0.4$, the correlation is assumed weak and ignored. The positive r_p presents a direct proportionality, while the negative r_p shows an inverse proportionality.

3. Results and discussion

3.1. Component comparison between synthetic and practical municipal wastewater

Table 2 shows the component comparison between synthetic and practical municipal wastewater. All insoluble components in

Table 2
Component comparison between SMW and PMW (mg/L) (n = 30).^a

	SMW		PMW	
	Soluble	Insoluble	Soluble	Insoluble
COD _{Cr}	200 ± 10	–	160 ± 30	20 ± 5
NH ₄ ⁺ -N	30 ± 1	–	26 ± 5	1 ± 1
TN	35 ± 2	–	30 ± 3	3 ± 1
TP	5 ± 1	–	3.5 ± 1.3	1.4 ± 0.5
Ca	38 ± 4	–	46 ± 8	67 ± 4
Mg	7 ± 3	–	8 ± 3	5 ± 3
Al	2 ± 1	–	0.5 ± 0.1	12 ± 13
Si	1 ± 1	–	30 ± 5	300 ± 30

^a Soluble and insoluble fraction of each element were separated with 0.45 μm membrane filter. Synthetic municipal wastewater was prepared with tap water and chemical, thus all components in SMW were soluble.

wastewater were remained effectively with reactor and membrane. Plenty of precipitate was accumulated at the bottom of reactor, thus regular bottom cleaning was needed for MBR-PW. Compared with insoluble components of wastewater, soluble components were easier for bacterial utilization. Higher soluble COD_{Cr} and NH₄⁺-N in SMW indicated that SMW contained richer nutrient, and lower concentration of COD_{Cr} and NH₄⁺-N in MBR-SW predicted the stronger material utilization efficiency. Additionally, inorganic element analysis with ICP indicated that Ca, Mg, Al and Si were the major inorganic elements in both SMW and PMW. Table 1 shows Si and Al, especially the insoluble parts, were the majority of the inorganic components in SMW. But SMW mainly contained soluble Ca as the major inorganic component. Tables 1 and 2 also present that membrane separation could not intercept soluble component with Ca and Mg, the majority of which flew out with effluent. Insoluble inorganic components with Ca, Mg, Al and Si were intercepted in MBR system with membrane separation. Therefore, the difference between PMW and SMW mainly led to the variations of inorganic components in the influent. In addition, compared with PMW, SMW offered richer nutrient for activated sludge in MBR system.

3.2. Cake layer morphology

Cake layer surface in MBR-SW and MBR-PW are shown in SEM images (E-supplementary data for this work can be found in e-version of this paper online). MBR-SW had a smooth cake layer surface with SMW, but the cake layer surface in MBR-PW was irregular. Previous studies (Zhou et al., 2015, 2014) reported that particles, especially the inorganic ones, in PMW accumulated easily onto cake layer surface during suction process. In other hand, Mg²⁺ addition in SMW even aggravated the sludge granulation to mitigate membrane biofouling, but the cake layer surface was still smooth (Sajjad and Kim, 2015). This predicts that the comparison between SMW and PMW would cause an obvious morphology variation of cake layer surface. Table 1 also shows that MBR-PW had lower MLVSS/MLSS rate than MBR-SW, indicating more inorganic components were in the MBR-PW, which was due to the inorganic component accumulation in the reactor. Therefore, components, especially the inorganic, in the influent play the significant role on the morphology of cake layer surface.

Fig. 1 further presents TMP and cake layer thickness variation between MBR-SW and MBR-PW. TMP increase rate is the index of cake layer formation process. The mathematical equation between day (x; day) and TMP (y; kPa) was, respectively, $y = 2.2x - 68.9$ ($R^2 = 0.9715$) and $y = 2.66x - 97.5$ ($R^2 = 0.9632$) in MBR-SW and MBR-PW. The higher slope in MBR-PW indicated that PMW induced severer membrane biofouling behavior. Fig. 1 also shows that MBR-PW had the thicker cake layer than MBR-SW. The correlated formula between day (x; day) and cake layer thickness (y; μm) was $y = 3.6x - 115.9$ ($R^2 = 0.9304$) and $y = 4.0x - 154.9$ ($R^2 = 0.9642$), respectively, in MBR-SW and MBR-PW, predicting that

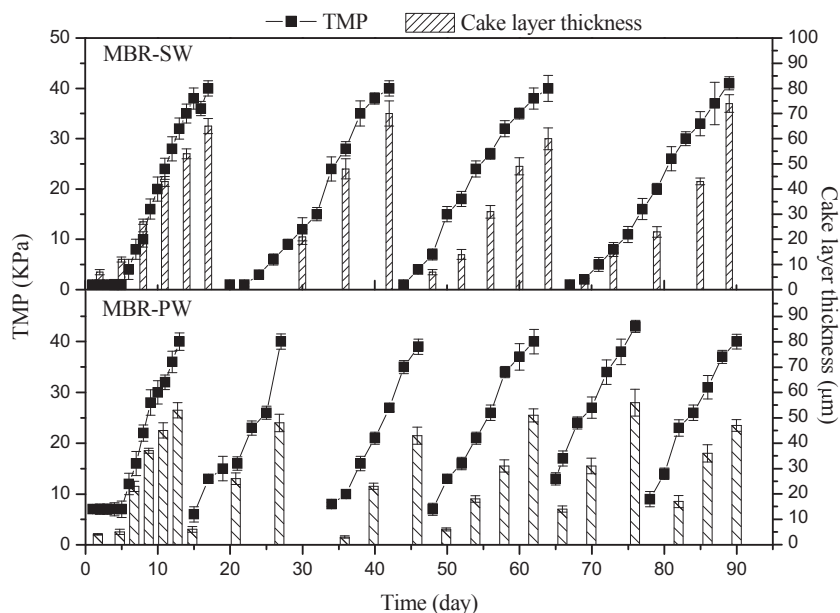


Fig. 1. Variations of TMP and cake layer thickness in MBR-SW and MBR-PW.

PMW aggravated cake layer formation. Consequently, PMW induced the severer membrane biofouling than SMW. In addition, Fig. 1 presents the relationship between TMP (x ; kPa) and cake layer thickness (y ; μm) in MBR-SW and MBR-PW was as $y = 1.6x - 0.2$ ($R^2 = 0.9288$) and $y = 1.5x - 10.1$ ($R^2 = 0.9464$), respectively. The gradient result indicated that the component variation in the influent had no obvious effects on the relationship between TMP and cake layer thickness.

3.3. Organic characteristics of cake layer

Table 3 shows that MBR-PW had the higher organic rate in the cake layer than MBR-SW, indicating that SMW promoted the organic components accumulated into cake layer. Additionally, ES, as the key organic mixture in cake layer, plays a significant role in cake layer formation (Guo et al., 2012; Zhang et al., 2008). Table 3 presents that ES variations between MBR-SW and MBR-PW. Polysaccharide, protein and TOC of ES in MBR-SW were higher than those in MBR-PW, which was because SMW contained lots of biodegradable components for bacterial metabolism and secretion (Villain et al., 2014). TMP growth had been considered as the index of membrane biofouling process (Zhou et al., 2014). Mathematical analysis of Table 3 results shows that r_p between organic rate and TMP was 0.68 and 0.54 in MBR-SW and MBR-PW, respectively, indicating that organic rate of cake layer had the positive correlation with membrane biofouling, which was consistent with previous studies (Meng et al., 2017; Zuthi et al., 2017), and indicated

Table 3

Polysaccharide (mg/g dry cake layer), protein (mg/g dry cake layer), and TOC (mg/g dry cake layer) of ES in cake layer, cake layer organic rate^a (%) and cake layer viscosity (mPa/s) ($n = 10$).

	MBR-SW	MBR-PW
Polysaccharide of ES in cake layer	42 ± 3	28 ± 2
r_p between polysaccharide and TMP	0.82	0.65
Protein of ES in cake layer	39 ± 5	26 ± 4
r_p between protein and TMP	0.51	0.47
TOC of ES in cake layer	122 ± 14	83 ± 8
r_p between TOC and TMP	0.65	0.56
cake layer organic rate	81 ± 4	72 ± 3
r_p between organic rate and TMP	0.68	0.54
cake layer viscosity	15 ± 2	7 ± 1
r_p between viscosity and TMP	0.53	0.46

^a Cake layer organic rate = organic components mass/total cake layer mass.

that SMW had a higher promotion on organic rate for membrane biofouling. Correlation coefficients between TMP and organic components (polysaccharide, protein and TOC) of ES in both MBR-SW and MBR-PW were > 0.4, predicting that organic components, especially polysaccharide, showed the direct positive proportionality with membrane biofouling. However, mathematical analysis also presented that PMW decreased the correlation coefficients between TMP and organic components of ES, meaning that organic behavior might be mitigated in MBR-PW. Cake layer organic rate decrease but severer membrane biofouling with PMW further indirectly proved the inorganic biofouling behavior enhancement in MBR-PW. Additionally, MBR-SW also had the higher cake layer viscosity (Table 3), which was due to higher organic component in cake layer. High viscosity of cake layer, having the positive correlation with membrane biofouling (0.53 and 0.46 in MBR-SW and MBR-PW, respectively), was one of the reasons for denser cake layer structure with SMW, especially humic substances (Kimura et al., 2005; Zhang et al., 2017).

Fluorescence spectra (Fig. 2) shows that Peak A (excitation/emission wavelengths of 270–285/320–330 nm), reported as tryptophan-like substances (Xia et al., 2015), was the major fluorescent organic component in cake layer. Tryptophan-like substance works as an important role in the bacterial metabolism (Schröcksnadel et al., 2006; Xia et al., 2015). As an α -amino acid applied in the biosynthesis of proteins, tryptophan-like substance is a measurement of biological activity through either bacterial production or algal growth and its grazing (Baker et al., 2007). Higher tryptophan-like substance in MBR-SW (Fig. 2) indicated activated bacterial behavior because of rich nutrient in SMW (Section 3.1). Additionally, there is no obvious variation of molecular weight (MW) distribution of ES in cake layer between MBR-SW and MBR-PW (Fig. 3), predicting that the comparison between SMW and PMW had no obvious effects on the MW distribution of ES in cake layer, even with rich nutrient in SMW. Moreover, only fraction ranging < 1 kDa of ES in MBR-SW were little higher than that in MBR-PW. Tryptophan-like substance is considered to be correlated with the autochthonous generation of small colloidal and dissolved organic matter in microbial activity (Baker et al., 2007). Thus, higher tryptophan-like substance in MBR-SW would lead to the < 1 kDa ES increase. In all, SMW highlighted the organic components in cake layer with bacterial metabolism promotion.

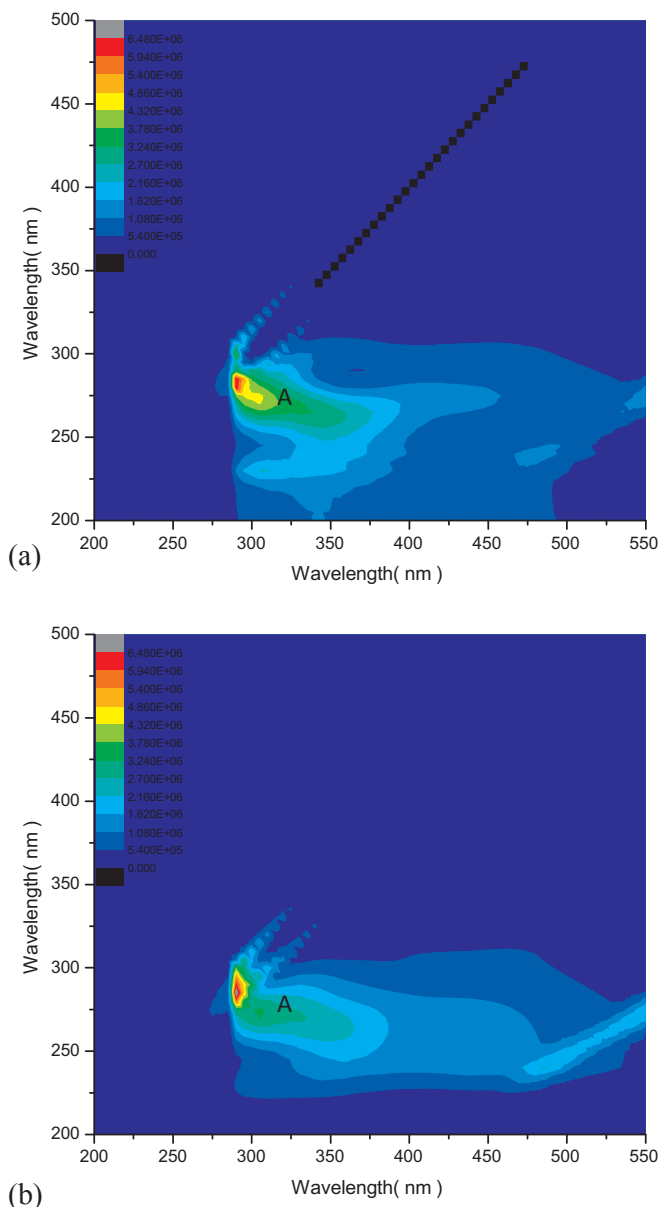


Fig. 2. Fluorescence spectra of ES in cake layer: (a) MBR-SW and (b) MBR-PW.

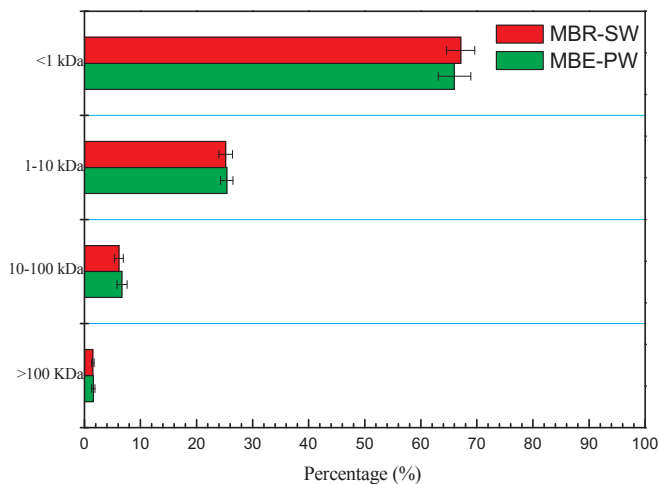


Fig. 3. MW distribution of ES of cake layer in MBR-SW and MBR-PW.

3.4. Inorganic characteristics of cake layer

XPS results shows that MBR-SW and MBR-PW had similar inorganic components in the cake layer, such as SiO₂, Al₂O₃, CaCO₃, CaSO₄ and Mg(II) (E-supplementary data for this work can be found in e-version of this paper online). Guo et al. (2012) has reviewed that inorganic components with Ca and Mg played the dominate role in cake layer structure, especially MBR for SMW treatment. SiO₂, Al₂O₃, CaCO₃, CaSO₄ and Mg(II) had been also reported as common inorganic components in activated sludge in MBR operation (Zhou et al., 2015), and thus the similar inorganic components in cake layer of both MBRs was because of the same inoculating sludge between MBR-SW and MBR-PW. Consequently, comparison between SMW and PMW would not induced obvious variation of inorganic form in cake layer. As a semiquantitative analysis, line scan EDX was carried out to identify element cross-sectional distribution in cake layer. As XPS results show, Si, Al, Ca and Mg were the major inorganic components of cake layer in both MBRs. SEM images shows that cross-sectional cake layer (inner structure) was smooth in MBR-SW, but that in MBR-PW was rough (E-supplementary data for this work can be found in e-version of this paper online). This result was consistent with cake layer surface SEM images.

Fig. 4 presents that MBR-SW and MBR-PW had the different distributions of Si and Al. Tables 1 and 2 show that PMW contained plenty of insoluble Si and Al, and most of them was remained in MBR reactor. Zhou et al. (2015) also reported that Si and Al were in the form of SiO₂-Al₂O₃ crystals in PMW and cake layer. Therefore, MBR-PW had similar Si and Al distribution along the cross-sectional cake layer, but MBR-SW contained lower Si and Al in its cake layer. However, because of ion form in SMW, Al was evenly distributed along cake layer in MBR-SW. Initial Si accumulation in both MBRs (Fig. 4(b)) was due to original Si components of sludge, and later Si accumulation in MBR-PW was mainly because of the Si in PMW. Additionally, inorganic components (especially Si), working as the framework of cake layer, intensify cake layer structure (Li et al., 2012; Zhou et al., 2015). In addition, mathematical analysis of correlation coefficient (r_p) (Table 4) shows that soluble Si and Al components in the influent had no direct correlation related to membrane biofouling in both MBRs. But the insoluble Si and Al substances in the PMW presented a high positive relationship with membrane biofouling, meaning that insoluble Si and Al directly lead to membrane biofouling. Consequently, inorganic components (especially Si) in PMW strengthened cake layer with denser structure, leading to severer membrane biofouling (Fig. 1). However, Fig. 4(c) and (d) shows that Ca and Mg, respectively, had the similar distribution along the cross-sectional cake layer in both MBRs, indicating that the comparison between SMW and PMW had no obvious effects on Ca and Mg accumulation onto cake layer. Results of Ca and Mg in the influent and effluent Tables 1 and 2) further indicated that few of Ca and Mg ions would accumulated into the cake layer. It indicated that Ca and Mg ions would be filtrated through membrane, or precipitate and deposit at the bottom of reactor, and only parts of precipitate and ions accumulated into cake layer (Zhou et al., 2015). Mathematical analysis of correlation coefficient (r_p) (Table 4) also shows that soluble Ca and Mg, and insoluble Mg did not have the obvious effects on membrane biofouling, compared with insoluble Si and Al. Additionally, although insoluble Ca had the high r_p with membrane biofouling with PMW, higher concentration of Si in PMW weakened the membrane biofouling contribution of insoluble Ca in MBR operation (Arabi and Nakhla, 2009; Zhou et al., 2015). Consequently, comparison between SMW and PMW mainly induced the variation of Si and Al, strengthening cake layer structure and causing denser cake layer.

4. Conclusion

This study identified comparison between SMW and PMW in cake layer characteristic analysis of MBR. PMW led to rough cake layer

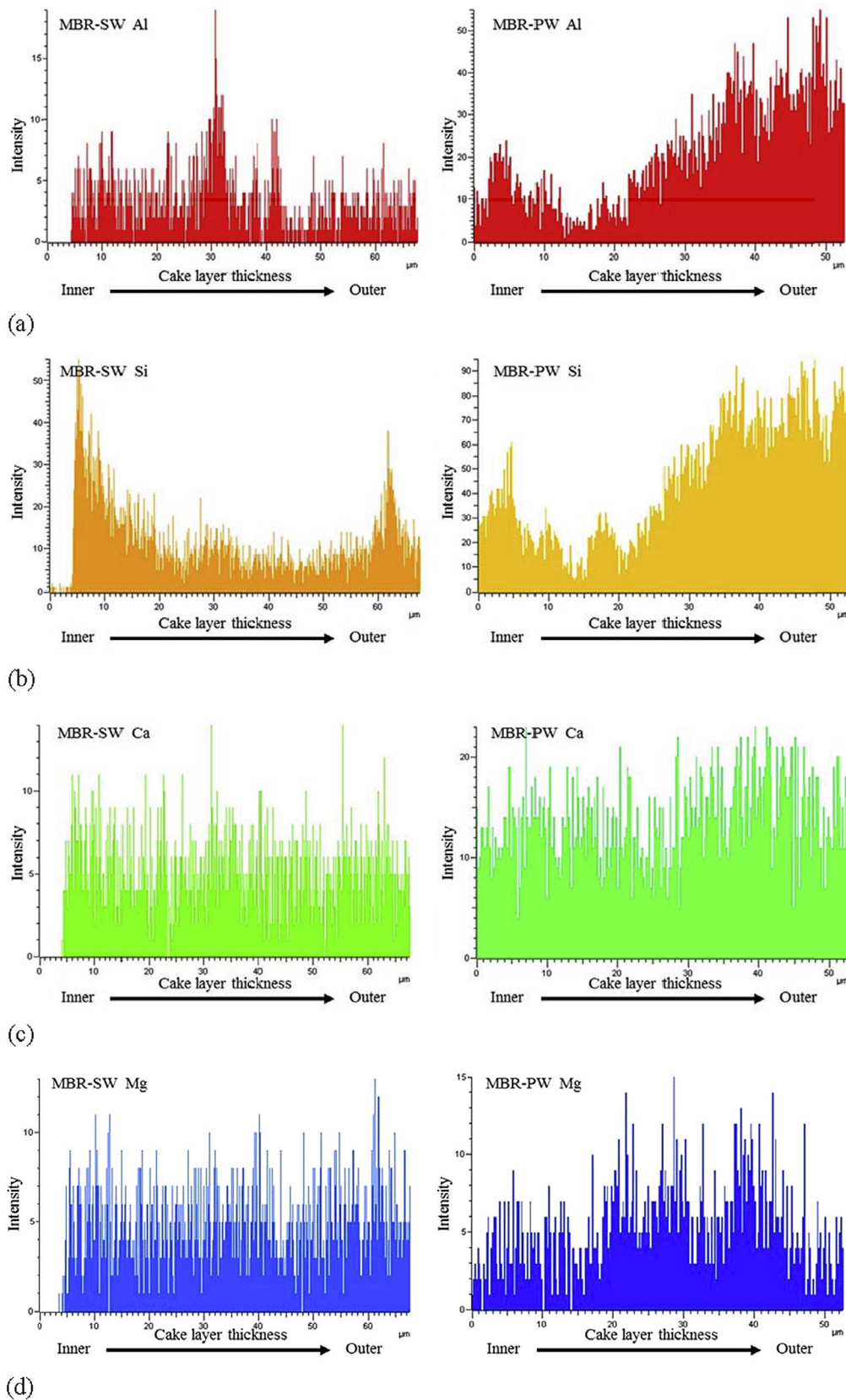


Fig. 4. (a) Al, (b) Si, (c) Ca and (d) Mg distribution along the cross-sectional cake layer in MBR-SW and MBR-PW.

surface with particles, and the aggravation of cake layer formation with thinner but denser cake layer. Inorganic components, especially Si and Al, in PMW accumulated into cake layer and strengthened the cake layer structure. SMW promoted bacterial metabolism

with rich nutrient, causing obvious organic accumulation onto cake layer. Therefore, SMW highlighted the organic components in cake layer, but weakened the inorganic functions in practical MBR operation.

Table 4

Correlation coefficient (r_p) between TMP and inorganic elements (Ca, Mg, Al and Si) in the influent. ($n = 10$).

	MBR-SW				MBR-PW			
	Ca	Mg	Al	Si	Ca	Mg	Al	Si
Soluble part in Influent	0.51	0.48	0.43	0.24	0.56	0.53	0.37	0.32
Insoluble part in Influent	–	–	–	–	0.61	0.48	0.72	0.83

Acknowledgements

This work is supported by the National Key Research and Development Plan of China (2017YFC0403403), Natural Science Foundation of China (NSFC 51678422), Foundation of State Key Laboratory of Pollution Control and Resource Reuse (Tongji University) (PCRR16003), and “the 111 Project”. In addition, W.-Q.Z. thanks the Catalyst: Leaders funding (CHN-UOA1601) provided by the New Zealand Ministry of Business, Innovation and Employment, and administered by the Royal Society Te Apārangi.

Appendix A. Supplementary data

Supplementary data associated with this article can be found, in the online version, at <http://dx.doi.org/10.1016/j.biortech.2017.08.069>.

References

Arabi, S., Nakhla, G., 2009. Impact of cation concentrations on fouling in membrane bioreactors. *J. Membr. Sci.* 343 (1–2), 110–118.

Baker, A., Elliott, S., Lead, J.R., 2007. Effects of filtration and pH perturbation on freshwater organic matter fluorescence. *Chemosphere* 67 (10), 2035–2043.

Campo, R., Capodici, M., Di Bella, G., Torregrossa, M., 2017. The role of EPS in the foaming and fouling for a MBR operated in intermittent aeration conditions. *Biochem. Eng. J.* 118, 41–52.

China-NEPA, 2002. *Water and Wastewater Monitoring Methods*, 4th ed. Chinese Environmental Science Publishing House, Beijing, China.

Dang, Y., Zhang, R., Wu, S.J., Liu, Z., Qiu, B., Fang, Y.L., Sun, D.Z., 2014. Calcium effect on anaerobic biological treatment of fresh leachate with extreme high calcium concentration. *Int. Biodeterior. Biodegrad.* 95, 76–83.

Deng, L.J., Guo, W.S., Ngo, H.H., Zhang, H.W., Wang, J., Li, J.X., Xia, S.Q., Wu, Y., 2016. Biofouling and control approaches in membrane bioreactors. *Bioresour. Technol.* 221, 656–665.

Du, X., Liu, G.Y., Qu, F.S., Li, K., Shao, S.L., Li, G.B., Liang, H., 2017. Removal of iron, manganese and ammonia from groundwater using a PAC-MBR system: the anti-pollution ability, microbial population and membrane fouling. *Desalination* 403, 97–106.

Duan, L., Jiang, W., Song, Y.H., Xia, S.Q., Hermanowicz, S.W., 2013. The characteristics of extracellular polymeric substances and soluble microbial products in moving bed biofilm reactor-membrane bioreactor. *Bioresour. Technol.* 148, 436–442.

Gkotsis, P.K., Mitrakas, M.M., Tolkou, A.K., Zouboulis, A.I., 2017. Batch and continuous dosing of conventional and composite coagulation agents for fouling control in a pilot-scale MBR. *Chem. Eng. J.* 311, 255–264.

Guo, W.S., Ngo, H.H., Li, J.X., 2012. A mini-review on membrane fouling. *Bioresour. Technol.* 122, 27–34.

Gurung, K., Ncibi, M.C., Sillanpaa, M., 2017. Assessing membrane fouling and the performance of pilot-scale membrane bioreactor (MBR) to treat real municipal wastewater during winter season in Nordic regions. *Sci. Total Environ.* 579, 1289–1297.

Homayonfal, M., Mehrnia, M.R., Rahmani, S., Mojtahedi, Y.M., 2015. Fabrication of alumina/polysulfone nanocomposite membranes with biofouling mitigation approach in membrane bioreactors. *J. Ind. Eng. Chem.* 22, 357–367.

Huang, L.Y., Lee, D.J., 2015. Membrane bioreactor: a mini review on recent R & D works. *Bioresour. Technol.* 194, 383–388.

Huang, P., Goel, R., 2015. Response of a sludge-minimizing lab-scale BNR reactor when the operation is changed to real primary effluent from synthetic wastewater. *Water Res.* 81, 301–310.

Jegatheesan, V., Pramanik, B.K., Chen, J.Y., Navaratna, D., Chang, C.Y., Shu, L., 2016. Treatment of textile wastewater with membrane bioreactor: a critical review. *Bioresour. Technol.* 204, 202–212.

Jiang, W., Xia, S., Liang, J., Zhang, Z., Hermanowicz, S.W., 2013. Effect of quorum quenching on the reactor performance, biofouling and biomass characteristics in membrane bioreactors. *Water Res.* 47 (1), 187–196.

Kimura, K., Yamato, N., Yamamura, H., Watanabe, Y., 2005. Membrane fouling in pilot-scale membrane bioreactors (MBRs) treating municipal wastewater. *Environ. Sci. Technol.* 39 (16), 6293–6299.

Li, Z.Y., Yangali-Quintanilla, V., Valladares-Linares, R., Li, Q.Y., Zhan, T., Amy, G., 2012. Flux patterns and membrane fouling propensity during desalination of seawater by forward osmosis. *Water Res.* 46 (1), 195–204.

Liu, S., Yang, X., Wang, B., Wang, W., 2011. Modeling of Membrane Fouling Based on Extracellular Polymers in Submerged MBR. *Procedia Eng.* 15.

Meng, F.G., Zhang, S.Q., Oh, Y., Zhou, Z.B., Shin, H.S., Chae, S.R., 2017. Fouling in membrane bioreactors: an updated review. *Water Res.* 114, 151–180.

Ng, K.K., Lin, C.F., Lateef, S.K., Panchangam, S.C., Hong, P.K.A., Yang, P.Y., 2010. The effect of soluble microbial products on membrane fouling in a fixed carrier biological system. *Sep. Purif. Technol.* 72 (1), 98–104.

Ou, S.H., You, S.J., Lee, Y.C., 2010. Extracellular polymeric substance characteristics and fouling formation mechanisms in submerged membrane bioreactors. *Desalin. Water Treat.* 18 (1–3), 175–181.

Sajjad, M., Kim, K.S., 2015. Influence of Mg^{2+} catalyzed granular sludge on flux sustainability in a sequencing batch membrane bioreactor system. *Chem. Eng. J.* 281, 404–410.

Schröcksnadel, K., Wirleitner, B., Winkler, C., Fuchs, D., 2006. Monitoring tryptophan metabolism in chronic immune activation. *Clin. Chim. Acta* 364 (1), 82–90.

Tian, Y., Su, X.Y., 2012. Relation between the stability of activated sludge flocs and membrane fouling in MBR: under different SRTs. *Bioresour. Technol.* 118, 477–482.

Villain, M., Bourven, I., Guibaud, G., Marrot, B., 2014. Impact of synthetic or real urban wastewater on membrane bioreactor (MBR) performances and membrane fouling under stable conditions. *Bioresour. Technol.* 155, 235–244.

Wang, Z.W., Wu, Z.C., Tang, S.J., 2009. Extracellular polymeric substances (EPS) properties and their effects on membrane fouling in a submerged membrane bioreactor. *Water Res.* 43 (9), 2504–2512.

Xia, S.Q., Guo, J.F., Wang, R.C., 2008. Performance of a pilot-scale submerged membrane bioreactor (MBR) in treating bathing wastewater. *Bioresour. Technol.* 99 (15), 6834–6843.

Xia, S.Q., Zhou, L.J., Zhang, Z.Q., Hermanowicz, S.W., 2015. Removal mechanism of low-concentration Cr (VI) in a submerged membrane bioreactor activated sludge system. *Appl. Microbiol. Biotechnol.* 99 (12), 5351–5360.

Xiao, K., Xu, Y., Liang, S., Lei, T., Sun, J.Y., Wen, X.H., Zhang, H.X., Chen, C.S., Huang, X., 2014. Engineering application of membrane bioreactor for wastewater treatment in China: current state and future prospect. *Front. Environ. Sci. Eng.* 8 (6), 805–819.

Zhang, B., Sun, B.S., Jin, M., Gong, T.S., Gao, Z.H., 2008. Extraction and analysis of extracellular polymeric substances in membrane fouling in submerged MBR. *Desalination* 227 (1–3), 286–294.

Zhang, Q., Tan, G.H., Stuckey, D.C., 2017. Optimal biogas sparging strategy, and the correlation between sludge and fouling layer properties in a submerged anaerobic membrane bioreactor (SAnMBR). *Chem. Eng. J.* 319, 248–257.

Zhou, L., Xia, S., Alvarez-Cohen, L., 2015. Structure and distribution of inorganic components in the cake layer of a membrane bioreactor treating municipal wastewater. *Bioresour. Technol.* 196, 586–591.

Zhou, L., Zhang, Z., Xia, S., Jiang, W., Ye, B., Xu, X., Gu, Z., Guo, W., Ngo, H.-H., Meng, X., 2014. Effects of suspended titanium dioxide nanoparticles on cake layer formation in submerged membrane bioreactor. *Bioresour. Technol.* 152, 101–106.

Zuthi, M.F.R., Guo, W.S., Ngo, H.H., Nghiem, D.L., Hai, F.I., Xia, S.Q., Li, J.X., Liu, Y., 2017. New and practical mathematical model of membrane fouling in an aerobic submerged membrane bioreactor. *Bioresour. Technol.* 238, 86–94.